Advanced lab course for Bachelor's students

Experiment T12

Detection principles

February 2022

Contents

General rules of behavior

Before starting with the experiment on one of the most interesting and fascinating thing in the world, it is useful to define the rules that everyone of us has to follow inside and outside the laboratory. **Do not skip this part and do not forget it!**

- Before entering the lab, place the jackets in the dedicated room
- Do not leave food in the wardrobe room. In case you have no place where to leave the not strictly necessary things, ask the supervisors
- Do not touch the radioactive sources with your hands! There are tweezers to move them...
- Always remember your dosimeter that has always to be with you. Attach it to a pocket or wherever you find it comfortable close to your body and do not leave it on the desk or in the bag
- Follow the indication in these instructions so that the apparatus can be preserved intact
- Don't worry about speaking English with the tutors: not a single point will be deduced if you are not confident with the language
- In case you need the tutors for whatever important reason, do not be shy and contact them

And...

... if you believe, like we do, that particle detectors are really cool, come and ask for a thesis in this field: in our institute there are several opportunities!

1. Introduction

This experiment is designed to give you basic knowledge about the working principles of particle detectors. Figure 1.1 shows a cross-sectional view of the Compact Muon

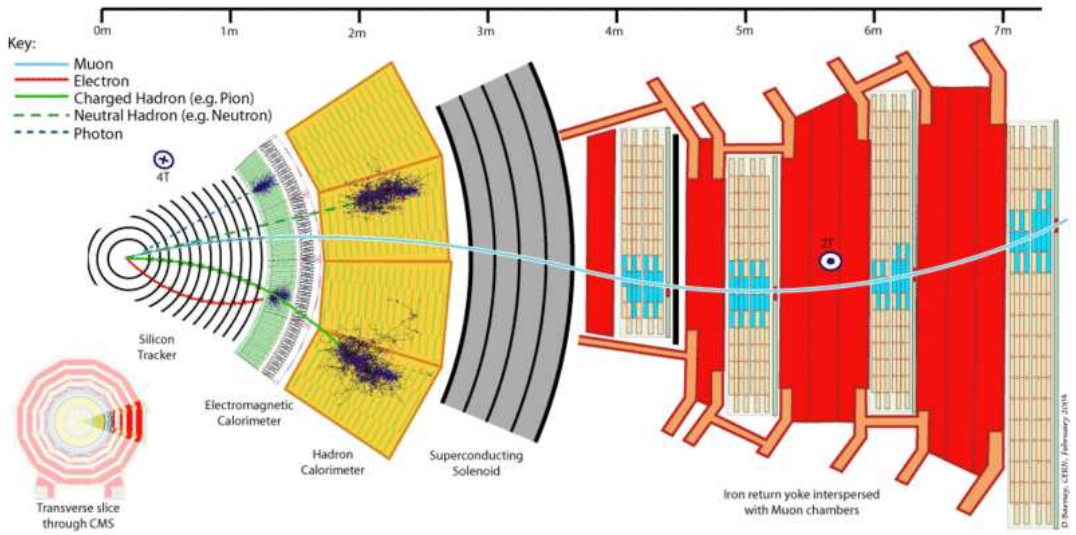

Figure 1.1.: Cross-sectional view of the CMS detector.

Solenoid detector, which is one of the four large experiments at the Large Hadron Collider. There are two basic ways of measuring particle properties.
First, a charged particle momentum may be measured by determining the curvature of its trajectory in a magnetic field. This is e.g. done in the so called tracker, which is a detector with a very good spatial resolution and allows for a precise trajectory measurement. The precision of this process is limited by the influence of multiple scattering due to the material present in the structure of the detectors, which causes a deflection of the particle path.
Second, a calorimeter can be used to measure the energy deposited by a traversing particle, that depends on the particle velocity. In CMS, there is an electromagnetic and a hadronic calorimeter. The electromagnetic calorimeter (ECAL) is used for the detection of photons and electrons/positrons, while the hadronic calorimeter (HCAL) is used to detect hadrons such as protons or kaons.
By determining the energy and the momentum, all the other properties of the particles can be derived, such as the mass and the p_T of the particles.

While in the LHC the particles crossing the detectors are produced making proton beams collide, in this laboratory experiment we will use electrons and positions (e^+, e^-) generated by the β-decay of radioactive sources.

2.1. β-decays

Nuclei with a large imbalance of proton and neutron content decay via the weak interaction. This decay is called β-decay. There are β^-- and β^+- decays, depending on the sign of the β particle generated:

$$n \rightarrow p + e^- + \tilde{\nu} \tag{2.1}$$
$$p \rightarrow n + e^+ + \nu \tag{2.2}$$

The first one occurs in neutron-rich nuclides. A neutron is transformed into a proton, which causes an electron and anti-neutrino to be emitted from the nucleus.
The opposite happen for proton-rich nuclei, which undergo β^+-decays. Here, a proton is transformed into a neutron and a positron and a neutrino are emitted. Energy corresponding to the mass difference between the parent nucleus and its decay products is released. This energy release is typically of the order of 1 MeV.

2.1.1. The β-spectrum

In contrast to the α-spectrum, the β spectrum is not discrete but continuous from zero to the maximal possible energy. The spectrum can be calculated from Fermi "Golden Rule", which describes the transition probability per unit time for a certain initial to final state process:

$$w = \frac{2\pi}{\hbar} \left| \langle \psi_f | \hat{H}_S | \psi_i \rangle \right|^2 \frac{dN}{dE_0} \tag{2.3}$$

$$\psi(\vec{r}) = \frac{1}{\sqrt{V}} e^{\frac{i\vec{p}\cdot\vec{r}}{\hbar}} \tag{2.4}$$

For the β-decay, the transition is from the initial nucleus to the final nucleus plus an anti-neutrino and free electron with a momentum between p_e and $p_e + dp_e$. The transition probability depends on the matrix element and the density $\mathrm{dN/dE_0}$ of possible final

states.
The weak interaction has a very short range and practically only affects the interior of the nucleus. Therefore, the wave function in the matrix element may be approximated using plane waves.

$$exp\left(\frac{i\vec{p}\cdot\vec{r}}{\hbar}\right) \approx 1 + i\frac{\vec{p}\cdot\vec{r}}{\hbar} - \frac{1}{2}\left(\frac{(\vec{p}\cdot\vec{r})}{\hbar}\right)^2 \tag{2.5}$$

Indeed, using $p_e \sim 1$ MeV/c and $r \sim 10^{-15}$ m, we get $\frac{\vec{p_e}\cdot\vec{r}}{\hbar} \approx 10^{-3}$. Assuming that the wave function is approximately constant over the extent of the nucleus, we can write:

$$\left|\langle\psi_f|\,\hat{H}_S\,|\psi_i\rangle\right|^2 = \frac{g^2\,|M_{fi}|^2}{V^2} \tag{2.6}$$

where g is a coupling constant that parametrizes the strength of the weak interaction and $|M_{fi}|$ is the nucleus matrix element containing the wave function. V is a normalizing factor for the wave function.
This equation tells us that electron and neutrino do not carry away any angular momentum. Thus, the transition is allowed (see below).
To calculate the density of allowed final states, we need to take into account that the released energy is shared between electron and neutrino: $E_0 = E_e + E_\nu$. Also, the total momentum of the system must be conserved. The nucleus is much heavier than electron and neutrino, which allows us to neglect the recoil energy carried by it. The total number of states dN is a combination of the electron and neutrino states:

$$dN = \mathrm{dn}_e\mathrm{dn}_\nu \tag{2.7}$$

where location and momentum are related by the uncertainty relation $d^3x d^3p \geq (2\pi\hbar)^3$. Each states occupies a phase volume of h^3, thus the total density of states is:

$$\frac{dN}{dE_0} = \frac{\mathrm{V}}{(2\pi\hbar)^3}4\pi p_e^2 dp_e\,\frac{\mathrm{V}}{(2\pi\hbar)^3}4\pi p_\nu^2\frac{dp_\nu}{dE_0} = \frac{16\pi^2\mathrm{V}^2}{(2\pi\hbar)^6}p_e^2 p_\nu^2\frac{dp_\nu}{dE_0}dp_e \tag{2.8}$$

where we have assumed that the interaction is confined to the volume V. This is possible due to the short range of the weak interaction. Neglecting neutrino masses, we arrive at

$$p_\nu^2 dp_\nu = \frac{(E_0 - E_e)^2}{c^3}dE_0 \tag{2.9}$$

and thus

$$dw(p_e) = \frac{2g^2}{(2\pi)^3\hbar^7 c^3}\,|M_{fi}|^2\,(E_0 - E_e)^2 p_e^2 dp_e = K\,|M_{fi}|^2\,p_e^2(E_0 - E_e)^2 dp_e. \tag{2.10}$$

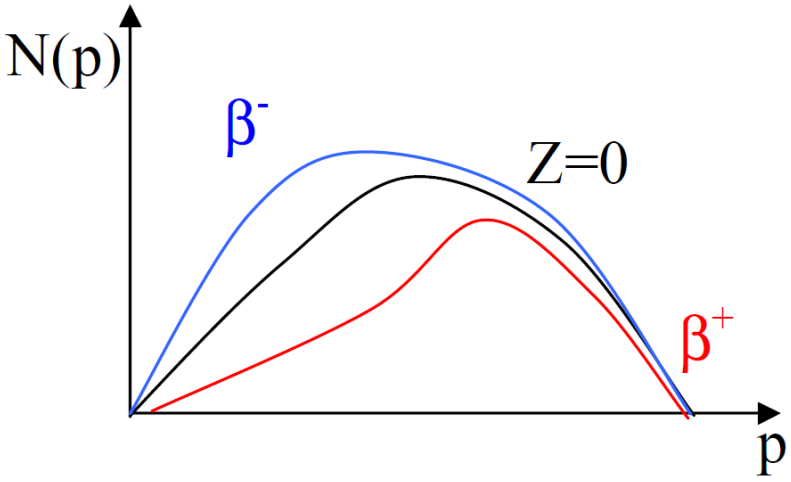

Figure 2.1.: Momentum spectrum with and without Fermi correction.

We can now replace E_e by the kinetic energy of the electron $T_e = E_e - m_e$ as it is measured in the scintillator and dp_e by dT_e, which gives

$$dw(T_e) = K\,|M_{fi}|^2\,(E_{max} - E_e)^2(T_e + m_e)\sqrt{T_e^2 + 2T_e m_e}dT_e \tag{2.11}$$

Note: In literature, it is common to only give the maximal kinetic energy of the electron E_{max} as decay energy.

2.1.2. Fermi correction

Up to this point we have neglected the Coulomb interaction between nucleon and electron/positron. When leaving the nucleon's electromagnetic field, electrons are decelerated and positrons are accelerated. The strength of this effect depends on the nucleon charge number Z and the momentum of the emitted particles. In both cases, the spectrum is distorted as shown in fig. 2.1. This correction is formulated as the ratio of the electron wave functions with and without the effect taken into account.

$$F(Z,\eta) = \frac{2\pi\eta}{1 - e^{-2\pi\eta}}\ ,\ \eta = \pm\frac{Z\alpha E_e}{p_e} \tag{2.12}$$

where + (−) is used for electrons (positrons). F(Z,p_e) is called Fermi function. The differential momentum distribution is then finally

$$\frac{dw}{dp_e} = K\,|M_{fi}|^2\,F(Z,p_e)p_e^2(E_{max} - E_e)^2. \tag{2.13}$$

2.1.3. Allowed and prohibited transitions

In all calculations, we have assumed the matrix element to be constant. However, this is only true for so called "allowed" transitions, where electron and neutrino do not carry angular momentum. Allowed transitions have high transition probabilities. There are two kinds of allowed transitions:

Fermi transition:
The spins of electron and neutrino are aligned in opposite directions. A singlet state ($s_\beta + \bar{s}_\nu = 0$) is formed, the nuclear spin is unchanged ($\Delta J = 0$).

Gamow-Teller transition:
Electron and neutrino form a triplet state ($s_\beta + \bar{s}_\nu = 1$). In this case, the nuclear spin may change by $\Delta J = \pm 1, 0$, where $J = 0 \to J = 0$ is excluded.

The other transitions are called "prohibited". The more prohibited they are, the more the rate is reduced. This means that the electron wave function is not constant over the extent of the nucleus as assumed in eq. 2.5. Therefore, the approximation has to be calculated in higher orders, which changes the matrix element. Whether a decay is prohibited, may be found out by considering the total decay probability per unit time λ. It is calculated by integrating the momentum spectrum over all possible momenta:

$$\lambda = \frac{1}{\tau} = \int_0^{p_{max}} \frac{dw}{dp_e}\, dp_e = K\,|M_{fi}|^2 \int_0^{p_{max}} F(Z, p_e) p_e^2 (E_{max} - E_e)^2\, dp_e \tag{2.14}$$

We define the kinetic energy per electron mass $W_e = \frac{E_e}{m_e c^2}$

$$\lambda = K'\,|M_{fi}|^2 \int_1^{W_{max}} F(Z, W_e) \sqrt{W_e^2 - 1} (W_{max} - W_e)^2\, dW_e \tag{2.15}$$

The integral is also called Fermi integral $f(Z, W_{max})$. It only depends on the nuclear charge Z and W_{max}. We replace the mean lifetime by the half-life:

$$\lambda = \frac{\ln(2)}{t_{1/2}} = K'\ |M_{fi}|^2\ f(Z, W_{max}). \tag{2.16}$$

And we thus arrive at the so called "ft value"

$$f(Z, W_{max}) t_{1/2} = \frac{\ln(2)}{K'\ |M_{fi}|^2}\,, \tag{2.17}$$

which may be used to estimate which class of transition a decay belongs to. It only depends on the matrix element. The value of the Fermi integral $f(Z, W_{max})$ for different

Z and W_{max} can e.g. be found in A.2 in the appendix.
ft values up to 10^6 are considered allowed, larger values are prohibited. The degree of prohibition (single, double, etc.) increases approximately every two orders of magnitude.

What kind of transitions are found in ^{90}Sr and ^{90}Y? ... we are going to use the ^{90}Sr in our experiment!

2.1.4. Kurie diagram

We can now plot $\sqrt{\frac{dw/dp_e}{F(Z,p_e)p_e^2}}$ against the electron's kinetic energy. If $|M_{fi}|^2$ is indeed constant, we expect a linear behavior as shown in 2.2. In this view, the maximal energy is determined by finding the intersection with the x-axis. Additionally, this plot can be used to spot multiple decay components in the spectrum, which lead to kinks in the line.

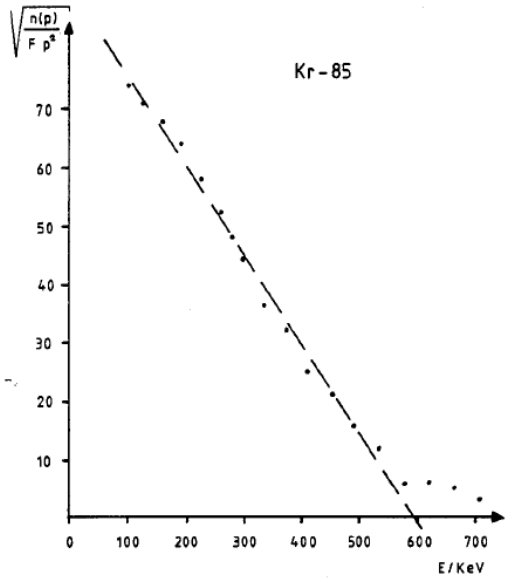

Figure 2.2.: Example Kurie diagram for the energy spectrum of Kr85.

2.2. Bending charged particles in magnetic fields

When an electrically charged particle traverses an electromagnetic fields, it is accelerated as shown in the Lorentz equation 2.18.

$$\vec{F} = q\ (\vec{E} + \vec{v} \times \vec{B}) \tag{2.18}$$

Where q is the particle charge, $\vec{v}$ is its velocity and $\vec{E}$ and $\vec{B}$ are the electric field strength and the magnetic flux density.

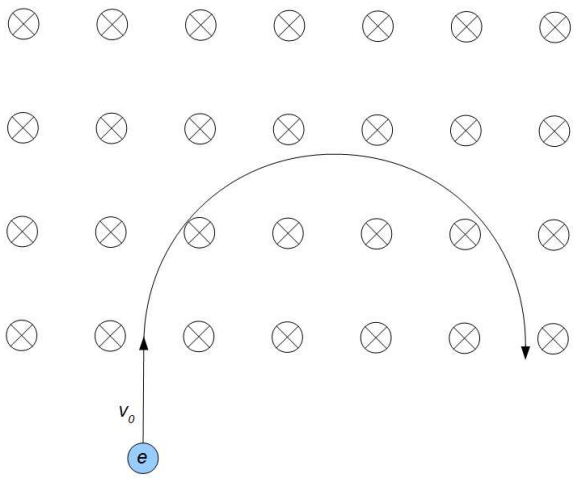

Figure 2.3.: Electron in a constant homogeneous magnetic field

The first term represents the Coulomb force $\vec{F_C}$. It linearly accelerates the particle (anti-) parallel to the field vector $\vec{E}$, depending on the particle's charge sign. The second term, called Lorentz force $\vec{F_L}$, is proportional to the particle charge and velocity. Due to the vector product, the resulting Lorentz force is orthogonal to the plane defined by $\vec{v}$ and $\vec{B}$. Thus, the particle path is deflected laterally, reaching the maximal value of deflection when velocity and magnetic field vectors are orthogonal and vanishes if they are parallel. A constant magnetic field does not alter the particle energy. To understand this, consider the following:

$$dW = \vec{F} \cdot d\vec{r} = \vec{F} \cdot \vec{v}\ dt = q\ (\vec{v} \times \vec{B}) \cdot \vec{v}\ dt = 0 \tag{2.19}$$

This equation tells us that the kinetic energy and, therefore, the velocity of the particle do not change when it traverses a constant magnetic field.
Now what happens, when a particle enters a constant, spatially homogeneous magnetic field? The motion has a circular path (Fig. 2.3).
This is due to the Lorentz force, which acts as a centripetal force. The particle traverses the circular path with a frequency $\omega = \frac{q}{m}B$, which is called Larmor frequency.
For a constant magnetic field, only particles with a certain momentum can occupy circular orbits of a certain radius R_0. The dependency may be calculated by equating the Lorentz force with the general expression for centripetal forces

$$F_\perp = F_L \tag{2.20}$$
$$m\tfrac{v^2}{R_0} = qvB \qquad , \ (\vec{v} \perp \vec{B}) \tag{2.21}$$
$$\Rightarrow mv = p = qBR_0 \tag{2.22}$$

or in natural units:

$$\frac{p}{keV} = 0.3\frac{B}{mT}\frac{R_0}{mm} \tag{2.23}$$

As stated before, the Lorentz force does not perform work, it does not change energy and speed of the particle. However, the particle is accelerated in the magnetic field, which leads to the emission of synchrotron radiation. Charged particles that are accelerated in a direction that is orthogonal to their velocity vector ($\vec{v} \perp \dot{\vec{v}}$) radiate the power

$$P \sim \frac{q^2}{c^3}\gamma^4(\dot{v})^2 \tag{2.24}$$

Which influence does the emission of synchrotron radiation have?

2.2.1. Particle's momentum measurement in CMS and tracking detectors

The charged particles crossing the CMS detectors leave ionization signals that are reconstructed as hits (cross symbols in figure 2.4). Using these spatial information, a track can be reconstructed by fitting the points with an helix-line. In the transversal view it assumes the shape of an arc of a circumference of length **L** and radius **R**. What is actually measured rather than the radius is the sagitta **s**, which is the maximal distance the track has from the straight line connecting the first and the last hits.

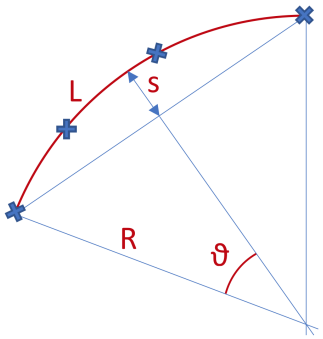

Figure 2.4.: Momentum measurement for charged particles in the CMS experiment.

Considering the θ angle small, the sagitta results:

$$s = R(1 - cos\theta) \approx \frac{R\,\theta^2}{2} = \frac{L^2}{8R} \tag{2.25}$$

So, obtaining R from the previous equation and substituting it into the generic momentum equation 2.23, we get the momentum equation depending on L, s and B:

$$p = 0.3\,B\,R \approx= 0.3\,B\,\frac{L^2}{8s} \tag{2.26}$$

2.3. Energy loss of electrons in matter

When particles traverse matter, they lose energy. This energy loss is caused by multiple effects. Particles may interact with shell electrons which causes excitations or even ionization. They may also interact with atomic nuclei, mostly by Coulomb scattering, which leads to the emission of Bremsstrahlung. If a charged particle travels at a speed higher than the speed of light in the corresponding medium ($c' = \frac{c}{n}$), Čerenkov radiation is emitted.
In this experiment, ionization and Bremsstrahlung are especially important. They are explained in more detail below.

2.3.1. Ionization

While the derivation of the formula of the energy loss for electrons and heavier particles in matter is different, the general approach is the same. Therefore, we will classically calculate the energy loss of heavy particles with $m \gg m_e$ by ionization and then the result will be translated for electrons. The derivation rests on the assumption that the energy of the incoming particle is much larger than the binding energy of the shell electron. Then, if the relative momentum transfer $\frac{\Delta p}{p}$ is small, the electron may be considered free and the trajectory of the heavy particle is a straight line.

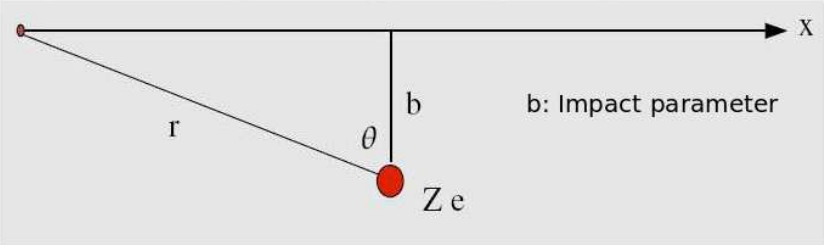

Figure 2.5.: Impact parameter definition.

When a particle with charge $Z_1 e$ passes close to the atom, the shell electron experiences a Coulomb force according to

$$\vec{F}_C = \frac{1}{4\pi\epsilon_0}\frac{Z_1 e}{(r^2)}\vec{e_r} \ . \tag{2.27}$$

The momentum transferred to the electron is

$$\Delta\vec{p} = \int_{-\infty}^{\infty} \vec{F}_C dt = \frac{e}{v}\int \vec{E}_\perp dx \tag{2.28}$$

where the longitudinal force component cancels because $\vec{F}_{C\parallel}(-x) = -\vec{F}_{C\parallel}(x)$. We use Gauss divergence theorem, obtaining

$$\Delta p = \frac{Z_1 e^2}{2\pi\epsilon_0}\frac{1}{bv}\ . \tag{2.29}$$

where b is the so called impact parameter, which quantifies the minimal distance between electron and incoming particle (see fig. 2.5).
The combined energy transfer to all electrons is calculated by integrating over all electrons in the volume dV. Using cylinder coordinates, we write

$$\Delta E = \frac{(\Delta p)^2}{2m_e} n_e dV = \frac{Z_1^2 e^4 n_e}{8m_e\pi^2\epsilon_0^2\beta^2c^2b^2}\, b\, d\phi db dx \tag{2.30}$$

where n_e is the electron density and $\beta = \frac{v}{c}$. The energy transfer per unit length is

$$\frac{dE}{dx} = \frac{e^4 Z_1^2 n_e}{4\pi\epsilon_0^2 m_e\beta^2c^2}\ln\frac{b_{max}}{b_{min}} \tag{2.31}$$

The maximal momentum therefore energy transfer is realized in central collisions, for which we obtain from eq. 2.29

$$\Delta p = 2m_e c\beta = \frac{Z_1 e^2}{2\pi\epsilon_0\beta c b_{max}} \tag{2.32}$$

$$\Rightarrow b_{max} = \frac{Z_1 e^2}{4\pi\epsilon_0 m_e c^2\beta^2} \tag{2.33}$$

The minimal energy transfer is the amount of energy necessary to ionize the electron. Therefore,

$$b_{min} = \frac{Z_1 e^2}{2\pi\epsilon_0\beta c}\frac{1}{\sqrt{2m_e I}} \tag{2.34}$$

where I is the mean ionization energy, which is about 163 eV for aluminum. For heavier elements, the average ionization energy may be approximated using

$$I = 9.73Z + 58.8Z^{-0.19}\text{eV}, \tag{2.35}$$

or for composites

$$\ln I = \sum_k g_k \ln I_k \tag{2.36}$$

where g_k is the ratio of electrons in atoms of kind k to the total number of electrons. Putting this into 2.31 yields

$$\frac{1}{\rho}\left(\frac{dE}{dx}\right)_{Ion} = \frac{Z_1^2 e^4}{8\pi\epsilon_0^2 m_e c^2}\frac{1}{\beta^2}\frac{Z}{A}N_A \ln\left(\frac{2m_e\beta^2c^2}{I}\right) \tag{2.37}$$

for the energy loss per unit length in $[\frac{dE}{dx}]$ = MeV cm^2/g. The electron density was replaced by $n_e \approx \frac{Z}{A}\rho N_A$, where A is the nucleus mass number and Z is the nuclear charge of the traversed material, which has a density ρ. The equation tells us that the energy loss depends on the speed ($\propto \frac{1}{\beta^2}$) and charge ($\propto Z_1^2$), but not the mass of the particle. The traversed material is considered in the factors $\frac{Z}{A}$ and $\ln(\frac{1}{I})$. Since scattering is a stochastic process, the formula only gives the average energy loss per unit length.
Now what changes when the incoming particle is an electron? Since the scattering partners are now equally heavy, the incoming particle does not follow a linear trajectory. Also, the scattering partners are quantum-mechanically identical particles, which makes a matching between initial and final state particles impossible. Here, we use the formula developed by Rohrlich and Carlson in 1954. It expands on work by Bethe.

$$\left(\frac{dE}{dx}\right)_{ion} = \frac{2\pi N_A r_0^2 m_e c^2}{\beta^2}\frac{Z\rho}{A}\left(\ln(\frac{\tau^2(\tau+2)}{2(I/m_e c^2)^2}) + \frac{\tau^2/8 - (2\tau+1)\ln 2}{(\tau+1)^2} + (1-\beta^2) - \delta\right) \tag{2.38}$$

Where $r_0 = \frac{e^2}{4\pi\epsilon_0 m_e c^2}$ is the classical electron radius and τ is the kinetic energy of the primary electron divided by $m_e c^2$, or simply $\tau = \gamma - 1$. δ is a density correction factor that represents the polarisation of the material caused by the electric charge of the traversing particle. For large distances, this causes a screening of the shell electrons. This effect is important for large energies and reduces the energy loss of the electron.

2.3.2. Bremsstrahlung

When charged particles are accelerated in the Coulomb field of atom nuclei, they emit Bremsstrahlung radiation. The emission is suppressed by the particle mass and thus only plays a role for light particles such as electrons. The average energy loss per unit length due to Bremsstrahlung is

$$\left(\frac{dE}{dx}\right)_{Brems} = 4\alpha N_A \frac{Z^2}{A} r_e^2 \ln\left(\frac{183}{Z^{\frac{1}{3}}}\right) E = \frac{E}{X_0}, \tag{2.39}$$

$$X_0 = \frac{A}{4\alpha N_A Z^2 r_e^2 \ln\left(\frac{183}{Z^{\frac{1}{3}}}\right)} \tag{2.40}$$

where $\alpha = \frac{1}{137}$ is the fine-structure constant. The energy loss is proportional to the initial energy of the incoming electron. X_0, called radiation length, is commonly given in $\frac{g}{cm^2}$.

It is the length after which the energy of the electron is attenuated by a factor $1/e \approx 37\%$.

The energy loss by ionization rises logarithmically at high energies, while Bremsstrahlung increases linearly. Thus, above some critical energy E_C the energy loss is dominated by Bremsstrahlung. For electrons in materials that are heavier than aluminum the critical energy may be determined using

$$E_C = \frac{800MeV}{Z + 1.2} \tag{2.41}$$

For composite substances, the average energy loss may be calculated as a combination of the individual losses for each of the components weighted with the corresponding mass fraction.

$$\frac{dE}{dx}_{tot} = \sum_i w_i \left(\frac{dE}{dx}\right)_i \tag{2.42}$$

2.4. Multiple scattering

When a particle traverses matter, many scattering processes occur. Each of the scattering events may change the travel direction of the particle (Fig. 2.6). Charged particles mainly scatter with the Coulomb field of the nuclei. This process causes the collimated incoming particle beam to expand in the medium. This affects the possible resolutions in detectors. Momentum measurements depend on the bending radius of charged particles in magnetic fields, which again depends on a precise spatial resolution. Since the actual travel distance in the material is unknown, dE/dx measurements are also distorted.

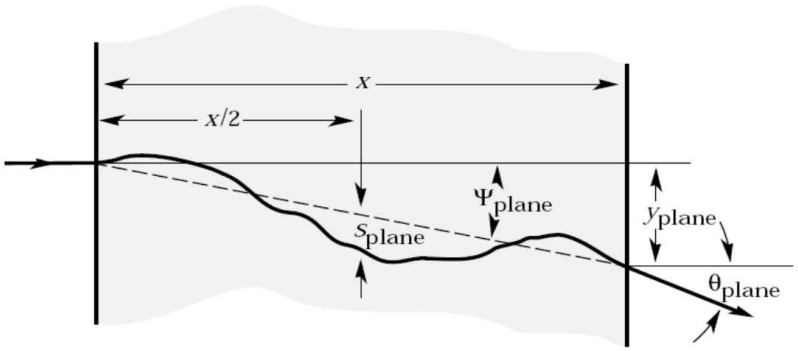

Figure 2.6.: Scattering in matter causes changes in travel direction of incoming particles.

This process is especially important for electrons. Their low mass facilitates large momentum transfers and thus large changes in travel directions. The effect of multiple scattering is described by Molière scattering theory. It states that the angular distribution is gaussian for small total scattering angles. This may be understood by thinking

of the total scattering angle as a superposition of many randomly distributed individual scattering angles. The Central Limit Theorem then states that the superposition is distributed according to a gaussian.
In this experiment, there are no mono-energetic electron sources, but a qualitative measurement of the effect may also be performed using a β-source.

The 3 experimental setups for this experiment are:

- Momentum resolution, Fig. 3.1;
- Energy loss in matter, Fig. 3.2;
- Multiple Scattering, Fig. 3.3.

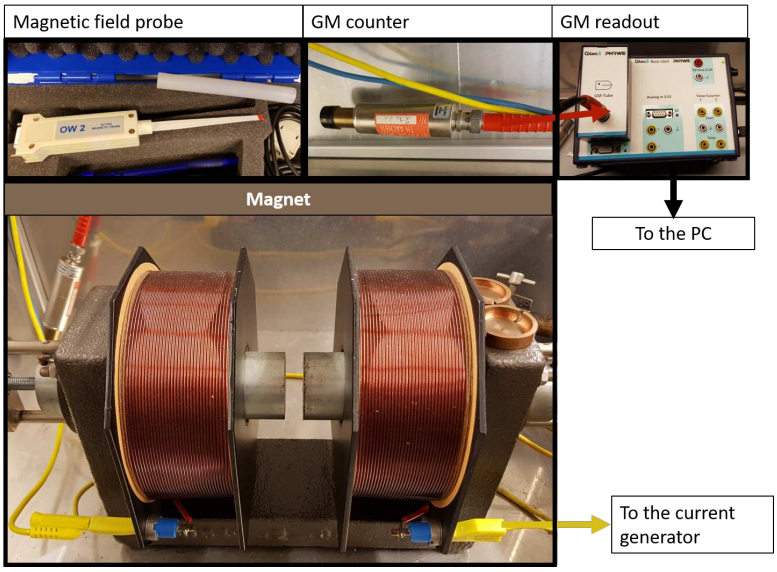

Figure 3.1.: Momentum resolution: experimental setup. The magnetic field produced by the magnet is controlled by mean of the current generator. The GM counts are read by the PC.

3.1. Detection devices for nuclear radiation

In this experiment, you are going to use two ways of measuring electrons emitted by the ^{90}Sr source: a Geiger-Müller counter and a scintillator. In the following sections, both detectors are explained.

3.1.1. Geiger-Müller counter

Geiger-Müller (GM) counters are among the oldest types of detection devices for nuclear radiation. They consist of a metal cylinder serving as a cathode and a thin wire inside

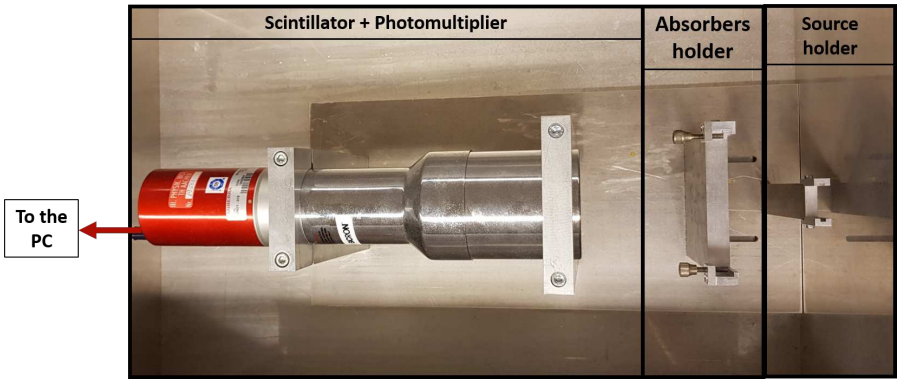

Figure 3.2.: Energy loss in matter: experimental setup. The PC controls both the photomultiplier HV settings and its current readout.

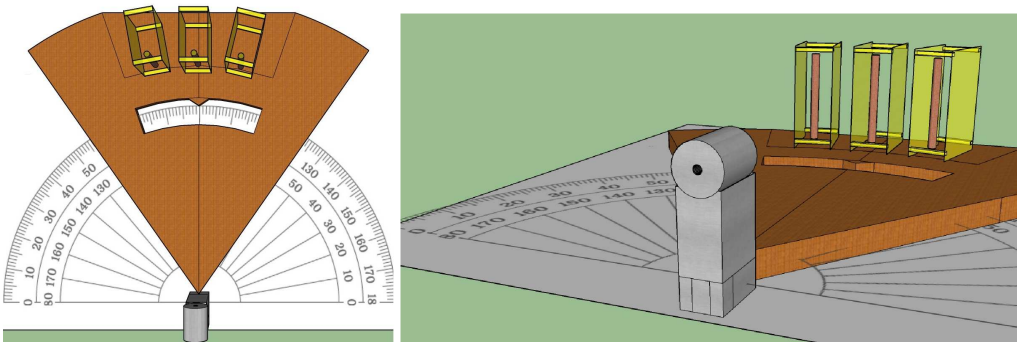

Figure 3.3.: Multiple Scattering: experimental setup - top and side view. Three GM counters (brown cylinders in the yellow cases) mounted on a support (brown) that can rotate around a pivot point. The radioactive source is placed inside the collimator (grey) above the pivot point.

the cylinder serving as an anode. Modern GM counters have a window covered with a low-mass layer (e.g. mica), which improves the detection efficiency. The cylinder is filled with a counting gas, which is a combination of a noble gas and a so called quenching gas. When ionizing particles traverse the volume, the gas is ionized along the particle path. The free electrons move towards the anode and cause a measurable current.
Depending on the applied voltage, the counter may be used in different ways.

The different working points are shown in fig. 3.4. In the recombination region, most electrons recombine with gas positive ions before reaching the anode. Above the recombination region, the counter may be used as an ionization chamber. Here, all electrons reach the anode and the measured current is proportional to the energy deposition of the ionizing particle.
At higher voltages, the proportional and gas amplification regions are reached. The strong electric field close to the anode accelerates the electrons in such a way that they again ionize the gas. The measured current pulse is still proportional to the energy deposition, but it is amplified. Proportional counters can be used to distinguish α- and

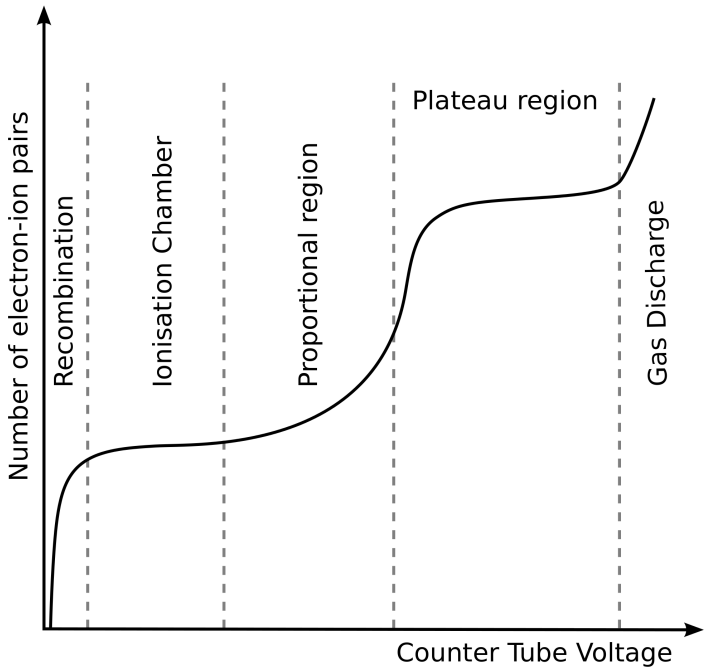

Figure 3.4.: Different operation regions of counter tubes.

β-radiation.
At even higher voltages, the amplification becomes so strong that an ionization avalanche covers the whole volume. The discharged state persists until the cloud of gas ions has traveled far enough towards the cathode to screen the electric field. The quenching gas prevents an additional firing of the tube. The measured current is now independent of the energy deposition and all particles cause the same signal.
In this experiment, we use a GM counter, that is read out using a Cobra3 system. Voltage supply and signal output use a BNC cable. A voltage of 500 V is supplied.

3.1.2. Scintillators

Scintillators are among the most used detectors for nuclear radiation.

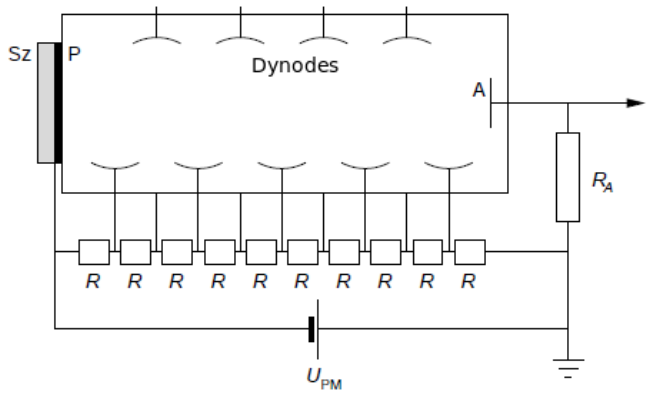

Figure 3.5.: Schematic drawing of scintillator and photomultiplier.

A schematic drawing is shown in fig. 3.5. In the scintillating material (Sz), ionizing radiation causes light flashes, which release electrons from the photo cathode P. Using a system of dynodes, which initiate emission avalanches, the number of photo-electrons is multiplied, thus amplifying the signal. The resulting voltage pulse is proportional to the energy deposition. The scintillation material should absorb as much of the energy of traversing particles as possible. The conversion fraction of traversing energy to light energy is called light yield. A linear relationship between the deposited energy amount and the number of scintillation photons is desirable to ensure a linear current response in the following. The scintillator should also be transparent to the scintillation light.

There are two types of scintillators with individual advantages. There are organic scintillator (e.g. plastic), which are very fast and only have small dead times. However, they have a bad energy resolution. Organic scintillators are commonly used as triggers for other detectors.
The second kind are inorganic scintillators such as NaI(Tl) or CsI, which have good energy resolution, but they are slow. In this experiment, a thallium doped sodium iodide scintillator is used. It has a very good light yield in the whole relevant spectral region (see fig. 3.6.
On the other hand, NaI(Tl) is fragile and hygroscopic, which makes insulation from air necessary. Due to their regular structure, inorganic crystals have pronounced band structure features. The scintillation process can thus be described using the band model (see fig. 3.7).
The valence band contains electrons bound to individual molecules, while the conduction band is filled with electrons which are free within the material. When energy is deposited in the crystal, electrons are lifted from the valence into the conduction band. When the electrons fall back to the valence band, a photon with energy E_1 is emitted. Since this energy corresponds to the difference between valence and conduction band

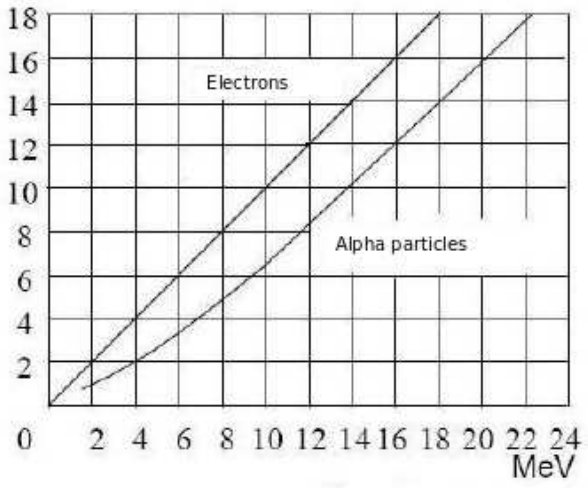

Figure 3.6.: Light yield of electrons and α-particles depending on their kinetic energy.

levels, the photon can be absorbed again. Thus, the material is opaque to the photon. To prevent this, activator atoms (here: thallium) are introduced into the crystal. The activator atoms cause additional energy levels close to the conduction band to be created. Electrons in the conduction band can now return to the valence band in two steps. They first fall into the activator states, which causes a phonon, but no photon to be created. In a second step they fall down from the activator states to the valence band, which causes emission of a photon. The photon now has an energy E_2 which is too small to cause additional excitations. The material is thus transparent to the photon.

3.2. Momentum resolution

This experiment is basically a momentum spectroscope, which is sketched in figure 3.8. Electrons are produced by the source S and pass through an opening of width Δx_1 into the magnetic field. Here, they are deflected and then detected using the detector D. In front of the detector, there is a cover with an opening of width Δx_2. Determine the momentum resolution assuming that electrons enter the magnetic field parallel to the x direction.

5;6800;1c

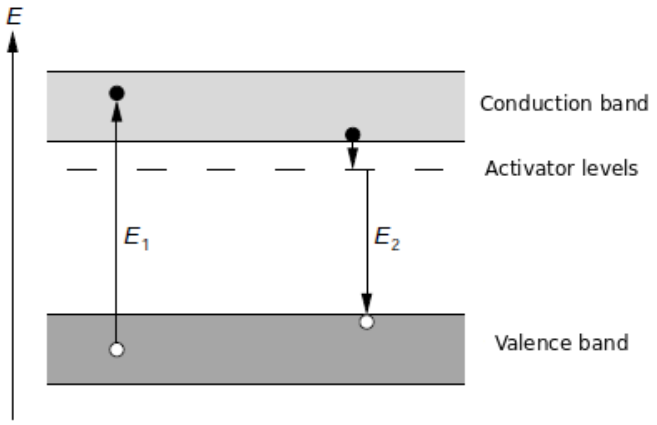

Figure 3.7.: Scintillation process of an inorganic scintillator visualized using the band model.

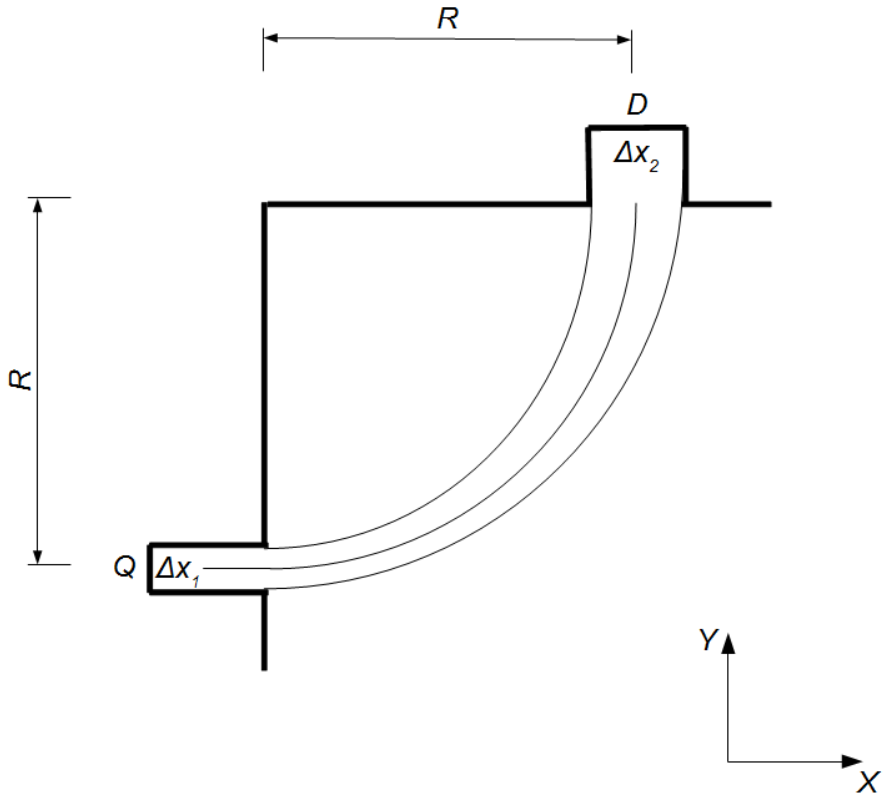

Figure 3.8.: Schematics of a momentum spectroscope.

4. Execution

4.1. Momentum measurement in a magnetic field

0. Always modify **slowly** the current feeding the coils of the magnet to reduce the probability to have residual magnetic field at zero current ($B_M = 0$ at $I_M = 0$). **The current must always be set to a value lower than $5\mathbf{A}$ ($I_M < 5\mathbf{A}$).** In addition, check that the aperture between the two poles of the magnet is less than 0.5 - 1 cm... Why?

1. Use the hall probe to measure the magnetic field between the pole pieces of the electromagnet; the grid drawn on the surfaces serve as a reference. Check where the magnetic field is homogeneous and how different currents affect the temporal behavior of the field. To do this, perform 60 seconds long measurements for different currents (sampling every 0.2 sec or whatever you find reasonable). **Attention**: connect the hall probe to the USB port on the right.

2. Use the available supplies to construct a setup for the measurement of the momentum spectrum of ^{90}Sr. Take care to choose a sensible and convenient position for source and GM counter. **Ask your supervisor to check the setup before putting it into operation!**

3. Measure the count rates in dependence of the magnetic field. Vary the field in appropriate steps. The settings of the power supply might be too coarse to vary the field as precisely as you would like. In this case, use the pole piece screw to adjust the field. Always keep the Hall probe into the aperture between the poles, in a fixed position OUTSIDE the electron path! If the value you get is slightly different from the one in the center of the magnet, you have to rescale it: use the field map measured in the point 1.

4. To estimate background levels, measure the count rate without a magnetic field. **Correct your measurement accordingly.**

5. Save your data before leaving the lab using a readable file format.

Note: The available hall probe works in transversal mode. Its measurement range is either $0 - 2$mT or $0 - 2$T. Depending on the chosen settings, it can measure constant or time dependent fields. Software to extract measured data is available.

4.2. Energy loss in matter

0. **Do not change the supply voltage (500V)**. Turn on the HV of the PM after having opened the program and turn it off before closing it.

1. When you collect the data, always check to have enough statistics. **Tip**: Save the data in .TKA extension, which corresponds to an easy readable text file...

2. Measure the spectrum of ^{90}Sr without any absorber. **Adjust the amplification factor such that the complete spectrum is recorded**.

3. Measure the spectra of ^{22}Na, ^{137}Cs, ^{60}Co and ^{152}Eu. These should enable you to do an energy-to-channel calibration.

4. Measure also the background... And use it properly!

5. Measure the spectra of the ^{90}Sr with the aluminium absorbers of different thicknesses (at least 4 $\rightarrow$ 0mm not included!).

4.3. Multiple scattering

The setup consists of 3 (or 4) GM counters read out by an Arduino - RaspberryPi chain. A sketch of the setup is shown in figure 3.3. Make the most out of the multiple GM counters on the setup, by chosing appropriate angular steps.

Run the following command on the RaspberryPi in order to read the counts:

```
python counter_number_only.py
```

This will give you insights on the rate with which you can evaluate the acquisition time for your measurement. When you are ready to start scanning the counts over the angle, run the following command:

```
python Auto_readout.py
```

Calibration

The GM counters have to be calibrated, since they do not return the same number of counts when exposed at the same particle flux. The tutors will provide calibration factors. The GM counters are already instelled their mounts. The radioactive source is placed inside the collimator (aluminum piece), can slide inside the collimator, but cannot pass through the openings.

Measurement of Multiple Scattering

1. By using a metal stick, push the radioactive source as far away as possible from the opening that faces the GM counters. This is the source *Position A*.

2. Measure the angular distribution of the electrons for the ^{90}Sr source without and with absorbers, choosing reasonable angular steps based on how you expect the distribution is. At least you should use 4 different thicknesses of aluminum and 4 different materials with the same thickness (compare it to the aluminum if it is not clear what is the size). Take care to choose sensible measurement times and consider the measurement of the background.

Measurement of the beam profile

The intensity and the collimation of the electrons beam hitting the GM counters, depend on the source positioning.

1. By using a metal stick, push the radioactive source as close as possible to the opening that faces the GM counters. This is the source *Position B*.

2. Measure the angular distribution of the electrons (beam profile) without absorbers. Choose reasonable angular steps based on how you expect the distribution is.

3. Restore the radioactive source back in *Position A*. Measure again the beam profile without absorbers in order to assess the reproducibility of the measurement.

Deadtime measurement of the GM counter

There is a spare Geiger-Mueller counter available to use for this part of the experiment. Therefore, please leave the GM counters attached to the apparatus within the aluminum shielding.

In this part of the experiment you will use an oscilloscope (in this case the Picoscope) to measure the analog signal output from the GM counter. From collecting these signals over some time window, one can measure the time between the initial signal pulse to the next pulse received. This is the deadtime, T_d, the window of time in which the gas detection volume needs to "reset" to be able to see a signal. This can be seen in Fig. 4.1. This first signal after the initial deadtime is smaller than the primary peak and subsequent signals recorded grow in amplitude. After some number of peaks, or additional time, the signal peak returns to it's original amplitude. The time in between the initial peak and the signal returning to this amplitdue is called the recovery time, T_r. You will measure the deadtime and recovery time of this GM counter.

To measure the deadtime, first confirm that the Picoscope is connected properly. To do this, first make sure that the USB cable is connected between the PC and the Picoscope. Next, connect the BNC connector of the probe into Output A. Then, connect the hook end of the probe lead to the leg of resistor R4 that is nearest the capacitor C2, as shown in Fig. 4.2. Also connect the ground lead of the probe to the GM voltage supply ground pin, also shwown in Fig. 4.2.

Next, confirm that the GM counter is connected to be powered by the Raspberry Pi or the Arduino. The 3.3 V pin of the GM counter needs to connect to the 3.3 V pin of the microcontroller. The ground pin should be connected to the microcontroller ground

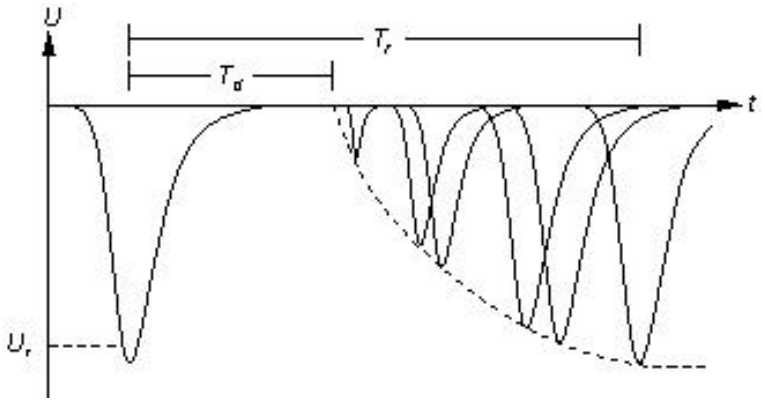

Figure 4.1.: An example Stever diagram showing the deadtime, T_d, and the recovery time, T_r of a sample detector.

pin. The GM counter pin locations are shown in Fig. 4.2. If you are unsure about the connections, confirm with the tutor prior to performing the experiment.

The settings listed in Table 4.1 should be used. The Persistance mode settings will be used later, you need not apply those at this point. We place them here for completeness and reference for later.

Table 4.1.: Settings associated with MightyOhm signal display using the PicoScope software. Some settings are only applied in *Persistence Mode*.

Settings	Values
Input range	± 2 V
Collection time	50 μs/div
Offset	-1.8 V
Resolution	16 bits
Trigger	
Trigger Mode	Repeat
Trigger	Simple
Edge Select	Rising Edge
Threshold	≈ -600 mV
Pre-Trigger	$\approx 5\%$
Persistence Mode only	
Mode	Digital Color
Saturation	$\approx 65\%$
Decayed Intensity	$\approx 15\%$

In the Appendix, there is a more in-depth discussion of the various settings for the Picoscope. If anything regarding the Picoscope software settings is unfamiliar or you are unsure about, check there first. To measure the output signal using the Picoscope, first confirm that you can read the output and get a single peak using the "Scope mode" of

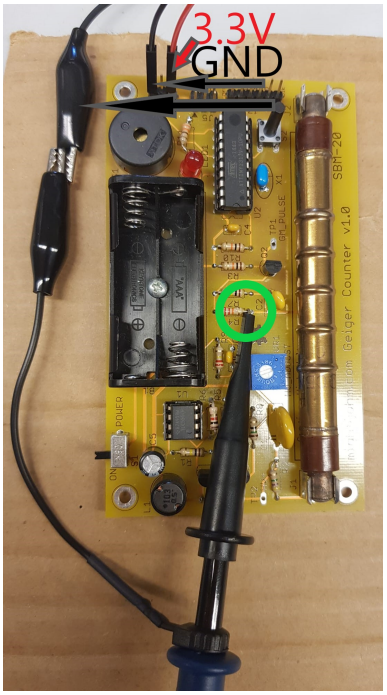

Figure 4.2.: Setup for the GM counter. The hook tip of the PicoScope probe is connected to the leg of the resistor *R4* which faces to the capacitor *C2* (green circle). The ground lead attached to the probe is connected to the ground of the voltage supply (crocodile clips on the right). Ground (black wire) and voltage (3.3V, red wire) are connected to the board (top). **Warning: High voltage is now present across the GM tube.**

the Picoscope. As a check, collect several events using comic ray muons as the source. The data collected by the Picoscope in this mode should appear similar to that in Fig. 4.3.

To find the deadtime, place the counter inside the aluminum volume such that the GM counter is within the acceptance region of the Sr-90 source. From here use the Persistance mode of the Picoscope software. The output in Persistance mode will show a color gradient based on the signal multiplicity (red=most common and blue=least common). This can be seen in Fig. 4.4. It can be helpful to suppress some of the gradient using the Phosphor option as shown in Fig. 4.5. As you can see, the gradient scale is suppressed, mostly leaving the signals that you are interested in allowing for easier determination of the deadtime and recovery time.

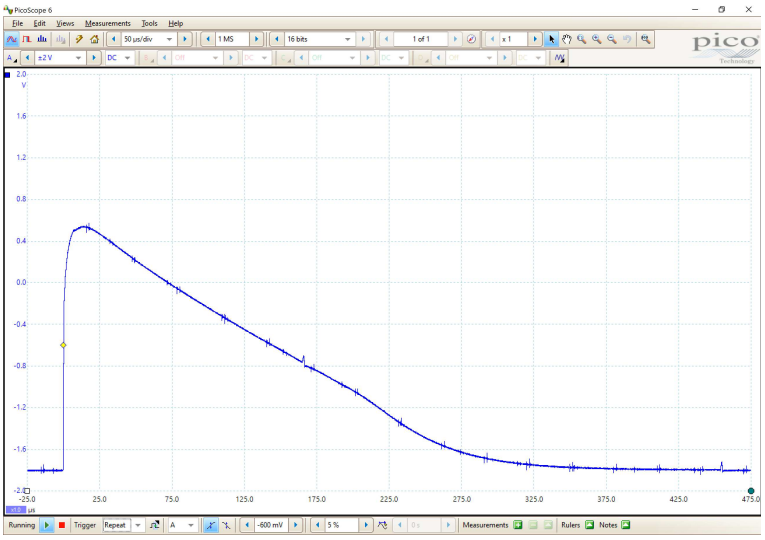

Figure 4.3.: A single GM counter pulse collected by the Picoscope.

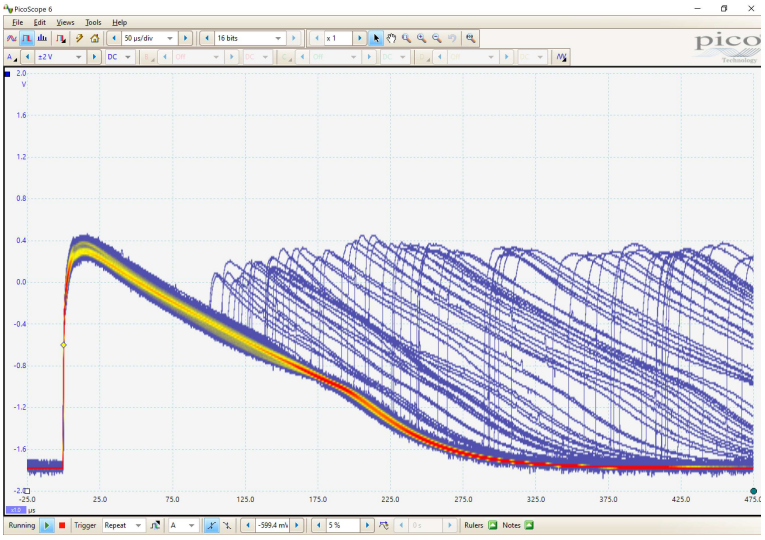

Figure 4.4.: The Persistance mode allows for generating the Stever diagram. In this mode a color gradient is present that corresponds to how freqent a signal is measured. Red shows most the common and blue the least.

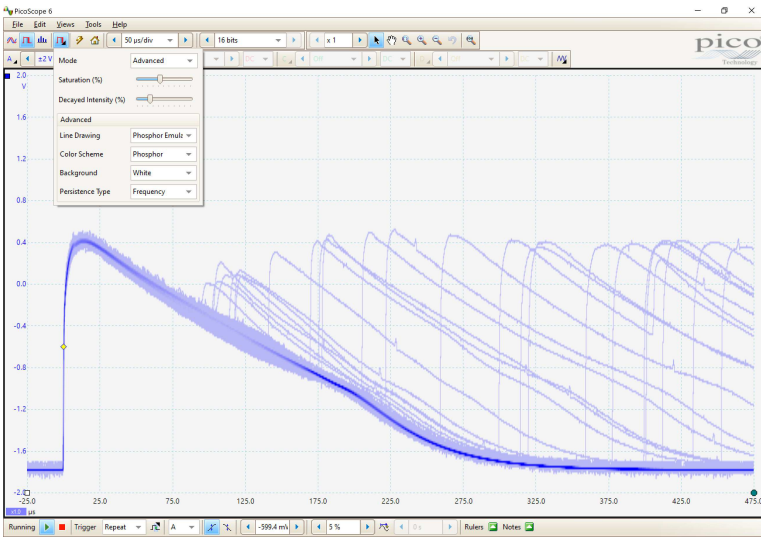

Figure 4.5.: In Persistance mode, using the Phosphor options it is possible to reduce the amount of signals that are not interesting allowing for a more accurate determination of the deadtime and recovery times.

5. Analysis

- Present the measured magnetic field properties appropriately and discuss them. Is the magnetic field sufficiently homogeneous or do you need to use an effective average? Where does the magnetic field become inhomogeneous?
- Plot the momentum and energy spectra. Transform the spectrum into a Kurie diagram, with and without Fermi correction. Use it to determine the maximal energy of the spectrum and estimate the uncertainty of $E_{\max}$. What effect does the Fermi correction have?
- Perform an energy-to-channel calibration for the scintillator.
- Plot the measured energy spectra. Present all spectra with aluminum absorbers in the same diagram. Do the same for the spectra with absorbers of the same strength. Once again, create Kurie diagrams and determine $E_{\max}$ and its uncertainty.

  The aluminum shielding has a nominal area mass density of $X = 147\frac{\text{mg}}{\text{cm}^2}$. The scintillator crystal is covered by an aluminum-oxide reflector with density $\rho = 3.94\text{g/cm}^3$. The reflector is meant to prevent scintillation photons from leaving the scintillation volume, thus increasing the light yield. It has a nominal thickness of 1.6 mm and an area mass density of $88\frac{\text{mg}}{\text{cm}^2}$. The reflector and aluminum shielding must be considered in the analysis of your data.

  - Compare your results to theory.
  - Are the nominal specifications correct?
  - Discuss your results.
- *Mutliple Scattering Measurement:* For each used absorbers, plot the rate measured by each GM counter versus your reference angle (position of the flag on the protractor). Are these angular distributions compatible with a gaussian distribution $gaus(A, \mu, \sigma)$? If yes, you have to normalize the rates of different counters: for the absorber *ab*:
  1. collect the fit parameters $\mu^{ab}_{GM1}, \mu^{ab}_{GM2}, \mu^{ab}_{GM3}, \mu^{ab}_{GM4}$;
  2. for each counter GMi rescale the point (refAngle, rate) $\rightarrow$ (refAngle -μ^{ab}_{GMi} , rate);
  3. plot all the rescaled points related to the absorber *ab* in the same diagram;
  4. fit these points with a gaussian distribution and collect the fit parameters $A^{ab}_{all}, \mu^{ab}_{all}, \sigma^{ab}_{all}$;

5. repeat steps 1-4 for all the used absorbers.

Consider the fit parameters obtained without absorbers (Air) and with the 4 thicknesses of aluminum.

1. Plot σ_{all}^{ab} versus thickness;
2. Plot A_{all}^{ab} versus thickness;

Describe quantitatively the results.

- *Deadtime and Recovery time Measurement:*
  1. From the Stever diagram, determine the deadtime and the recovery time of the GM counter.
  2. Do your results make sense? Support with reasoning.
  3. Is there are range for the rate for where the meausrement of a radioactive source is severely limited by the deadtime of this detector and one should use another detector. Why or why not?

- *Source Profile Measurement:* you have measured and fitted the angular distributions for two different source positions (*Position A* and *Position B*). Plot both angular distributions in the same diagram. What are the differences in the angular distributions and the beam rates between these positions? How can you explain them?

- Compare the two angular distributions you have measured for the source in *Position A* and fit them with a gaussian distribution. How much do the fit parameters differ each other? Is the difference caused by a statistical and/or systematic error?

- You have measured the maximal energy and momentum of charged particles. Calculate the particle mass! Discuss uncertainties. Can this result be used to identify the particles?

- Briefly discuss how these measurement methods are used in modern detectors. What does this tell us about a "good" detector?

- To what class does the transition from ^{90}Y to ^{90}Sr belong?

Many of the results from this experiment will have limited precision (e.g. the mass measurement). Your analysis should focus on correct handling of uncertainties. It should reflect your understanding of principles and methods. Many plots can be put into the same figure. Important results should be given in the text or in tables.

Appendices

A.1. Sources

The gamma emitters ^{22}Na, ^{137}Cs, ^{137}Co and ^{152}Eu are used for energy calibration. The used β-source is ^{90}Sr with activity of 1 MBq. The decay scheme is shown in fig. A.1.

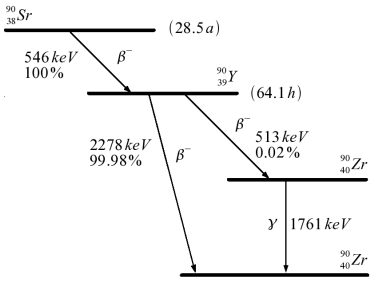

Figure A.1.: Decay scheme of ^{90}Sr.

A.2. Fermi integral

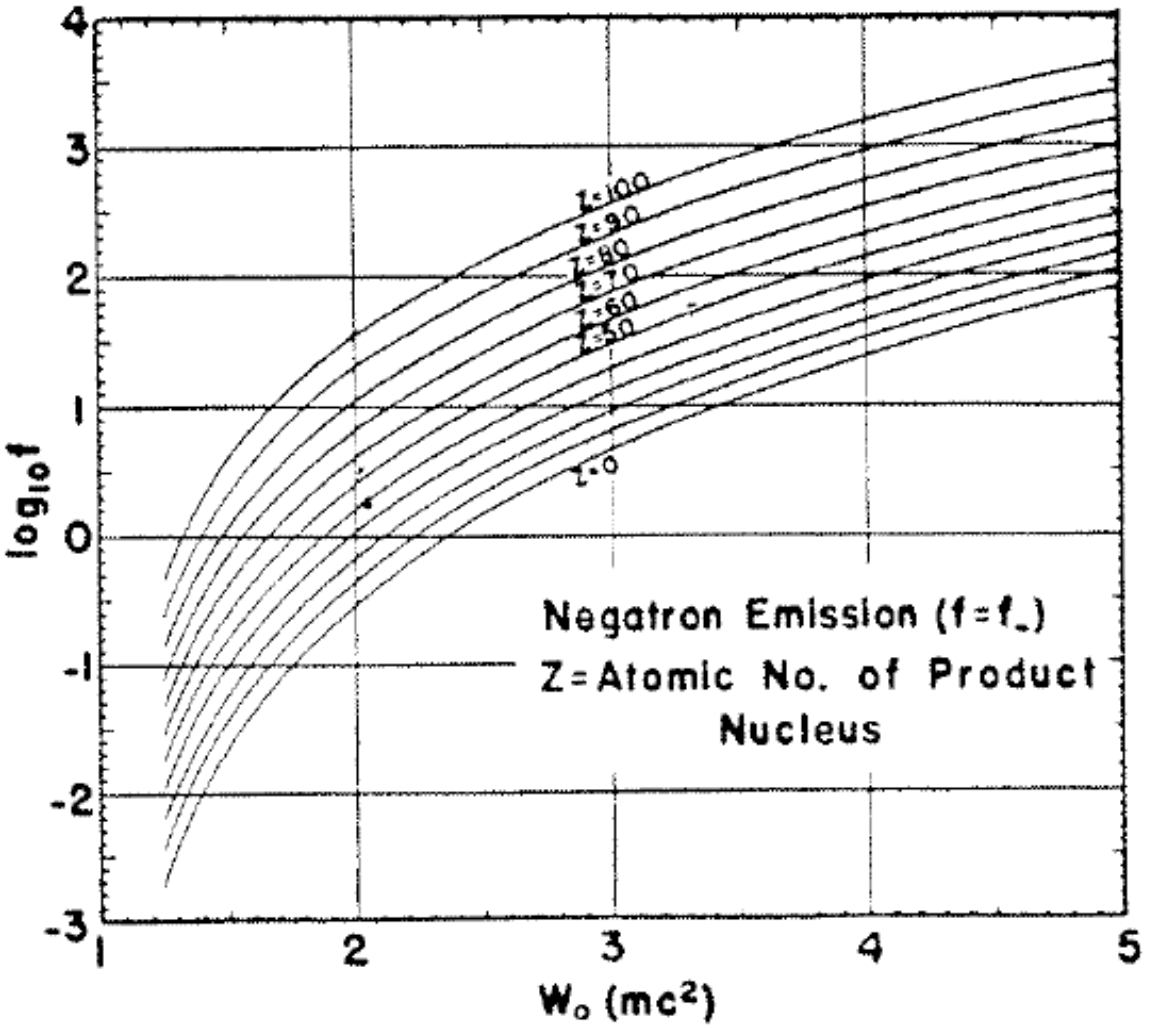

Figure A.2.: Logarithmic view of β^-decay spectra at different nuclear charges.

B. Charged particles in magnetic fields: equation of motion

In this appendix, we want to go though the computation of the equation of motion of a particle inside a constant magnetic field (Fig. 2.3).

Without loss of generality, we choose our coordinate system such that

$$\vec{v} = \begin{pmatrix} v_0 \\ 0 \\ 0 \end{pmatrix}, \ \vec{B} = \begin{pmatrix} 0 \\ 0 \\ B \end{pmatrix} \tag{B.1}$$

which gives us the equation of motion

$$m \ \ddot{\vec{x}} = q \ \vec{v} \times \vec{B} \tag{B.2}$$

with the initial conditions

$$x(0) = 0, \ y(0) = 0, \ \dot{x}(0) = v_0, \ \dot{y}(0) = 0 \tag{B.3}$$

where $t = 0$ is the time at which the electron enters the magnetic field. We suppress explicit time dependencies and write the separate components:

$$\ddot{x} = \frac{q}{m} B\dot{y} \tag{B.4}$$

$$\ddot{y} = -\frac{q}{m} B\dot{x} \tag{B.5}$$

This is a system of coupled differential equations. Performing time integration yields

$$\dot{x} = \frac{q}{m} By + C_1 \tag{B.6}$$

$$\dot{y} = -\frac{q}{m} Bx + C_2 \tag{B.7}$$

where the integration constants $C_1 = v_0$ and $C_2 = 0$ are determined from the initial conditions $\dot{x}(0) = v_0, \ y(0) = 0$ and $\dot{y}(0) = 0, \ x(0) = 0$. By putting eq. B.7 into B.4, the differential equations are de-coupled:

$$\ddot{x} = -(\frac{q}{m} B)^2 x \tag{B.8}$$

Equation B.8 describes a harmonic oscillation and is solved by

$$x(t) = A_1 \cos wt + A_2 \sin wt, w = \frac{q}{m} B \tag{B.9}$$

Using the initial condition $x(0) = 0$, we get $A_1 = 0$. Also, we deduce $\dot{x}(0) = v_0 \Rightarrow A_2 = \frac{v_0}{w}$ and arrive at

$$x(t) = \frac{v_0}{w} \sin wt \tag{B.10}$$

We put B.10 into B.7 and get

$$\dot{y} = -v_0 \sin wt \tag{B.11}$$

integrating one more time yields

$$y(t) = \frac{v_0}{w} \cos wt + C_3 \tag{B.12}$$

Where we have determined $C_3 = -\frac{v_0}{w}$ from $y(0) = 0$.

$$y(t) = \frac{v_0}{w}(1 - \cos wt) \tag{B.13}$$

The final solution is then

$$\vec{r} = \begin{pmatrix} x(t) \\ y(t) \\ z(t) \end{pmatrix} = \begin{pmatrix} \frac{v_0}{w} \sin wt \\ \frac{v_0}{w}(1 - \cos wt) \\ 0 \end{pmatrix} \tag{B.14}$$

As we expected, this equation of motion describes a circular path. This is due to the Lorentz force, which acts as a centripetal force.

C.1. Introduction of the PicoScope

[LE,RO]Introduction

C.1.1. Setup of the PicoScope

Hardware

Usually, the PicoScope oscilloscope can be used in the experiments without major changes to the existing experimental setup.
The power supply of the PicoScope oscilloscope is plugged in and the oscilloscope is connected to a PC via an USB cable. Four independent channels can be connected via the BNC connectors on the front. For instance, probes which are delivered with the PicoScope can simply be connected to such an input.
The used PicoScope model also features an output channel which can be adjusted with the software such that it outputs the defined function.
The described input and output connections are displayed in Figure C.1.

Software

On the homepage of pico Technology, the software PicoScope can be obtained which has to be installed to access and control the PicoScope oscilloscope. After starting the software, the PicoScope oscilloscope should connect automatically.

C.1.2. Using the software

The basics for operating the PicoScope software are explained in this section. Also some advanced features will be described as they proved useful in the actual experiments of the lab course.

General remarks

Depending on the context, it can be advantageous to save certain settings of the PicoScope in order to load them at a later time. This can be achieved at *File* → *Start-up Settings* → *Save Settings As...* and a setting file is accessed by either opening it in the Windows Explorer (if automatically associated with the PicoScope software) or use *File* → *Open*. In the menu *Start-up Settings* it is also possible to set default settings which are always loaded when starting the software or set the option to restore the settings of the last PicoScope session. The latter option is especially useful if one wants to continue with some work in the software after it was closed. Therefore, it is advised to activate this option as default settings if no user default settings are set.

Scope Mode and *Persistence Mode*

Two different view modes are used in the lab course. The *Scope Mode* shows the signal captured during the *Collection Time* once. The *Persistence Mode* overlays multiple recorded signals and fades out the signals with time. This behaviour can be associated with the afterglow of signals on an analog oscilloscope.
Both modes share many settings regarding the display of the signal (e.g. *Input Range* and *Offset*) which are explained in Section C.1.2. However, the *Persistence Mode* features additional settings to modify the afterglow effect. Most important are the *Mode* setting (cf. Fig. C.2) where *Digital Color* uses different colors to indicate how often a certain signal value occurs at a given time and *Analog Intensity* draws recent signals with full intensity while signals get paler with time. The options *Decay Time*, *Saturation* and *Decayed Intensity* define the time how long a signal takes to fade out, the intensity with which a new signal is drawn and the intensity at which signals remain after the decay time elapsed, respectively.
A special characteristic of the *Scope Mode* is the possibility to save waveforms not only as an image but also the data points in a csv or txt file. This is emphasized in Section C.1.2 and not possible in the *Persistence Mode*. It is also possible to view some previously captured signals which are stored in the buffer. Another view mode is the *Spectrum Mode* which uses a fast Fourier Transformation to display a spectrum view. As this mode is not used in the lab course currently, this feature is not covered here in further detail but information can be found in the PicoScope user's guide. Both view modes are shown in Figure C.2.

Changing the display of the input signal

The different options to modify the display of the signal are explained using Figure C.3. The green boxes show the options which apply to all channels.

(1) The *Collection Time* determines how long a capture of a signal lasts. Usually, the time is stated per division . The total time is derived by using a factor 10 for the number of divisions.
(2) The *Number of Samples* does only need attention in some cases. The number stated is an approximate value. In the menu *Views* → *View Properties*, the actual number of samples as well as the sampling interval can be seen. For many purposes the default set value of *Number of Samples* is sufficient but for short-lived peaks and large *Collection Times* the sample interval should be considered eventually.
(3) The *Hardware Resolution* can take values from 8 to 16 bits and determines the quality of the digitized signal. Note that 15 bits and 16 bits resolution are only possible if two and one channel, respectively, are used. Using the option *Auto resolution* is usually sufficient.
(4) The zoom functions can be used to enlarge a region of the scope and investigate the waveform closer without changing the *Input Range* or *Collection Time*.

The following options can be adjusted for each channel individually.

(5) The *Input Range* option determines the minimal and maximal input value for the channel. A channel can also be turned off. If the recorded signal is larger than the *Input Range*, a warning (Channel overrange) is displayed in the upper left corner and the input range should be increased.
(6) The *Coupling* can be set to AC or DC. In the AC mode, frequencies $\lesssim 1\,\mathrm{Hz}$ are filtered out. Therefore, DC offsets are not visible, allowing for more precise signal measurements but relative voltages with respect to the ground cannot be measured. In the DC mode, the signal is measured with respect to the ground.
(7) An *Analog Offset* can be applied to the input before digitization. This is useful cases where the maximum amplitude is known, e.g. if pulses with height 10 V are expected, the *Input Range* of $\pm 10\,\mathrm{V}$ does not have to be used but $\pm 5\,\mathrm{V}$ with an *Analog Offset* of $-5\,\mathrm{V}$.
(8) The *Axis Scaling* options can be used to manipulate the display of the signal. In contrast to the *Analog Offset*, these options apply to the axis not the signal.

Trigger

A plethora of triggers is available which are especially useful for finding rare and short-lived signals. The options are explained with Figure C.4. All options regarding trigger are set in the menu bar at the bottom of the software.

(1) Different *Trigger Modes* are available determining what signals are displayed. The most important are
   – *None*: No trigger is used.

  - *Auto*: Displays a triggered waveform but if no present the input signal is displayed regardless of the trigger.
  - *Repeat*: Displays only triggered waveforms.

(2) *Advanced Triggers* can be used but usually the *Simple Edge* trigger is sufficient which fires when the signal passes through a certain threshold. The other triggers have additional features, e.g. allowed voltage windows for the signal. The options (3)-(5) can also be adjusted in this context menu.
(3) Usually, the *Trigger Channel* is the same as the displayed signal. If multiple inputs are displayed, one channel has to be chosen which triggers for all inputs. It is also possible to trigger on an external channel.
(4) The *Edge Select* option allows to trigger on either falling or rising edges.
(5) The *Threshold* can be typed in at the menu bar, in the *Advanced Triggers* menu or by dragging the marker (yellow square in the scope) at the desired position.
(6) The *Pre-trigger* determines how much of the signal is captured and displayed before the trigger fires. It can also be adjusted by dragging the marker in the scope.
(7) The *Trigger-delay* has to be enabled by clicking on the respective item in the menu bar and determines how much time has to elapse before the trigger can fire again.

For most purposes, the *Simple Edge* trigger with a sufficient *Threshold* and *Pre-trigger* and correct *Edge Select* is sufficient.

Saving waveforms

The PicoScope software features the saving of captured waveforms either as an image or a csv/txt file if the *Scope Mode* is used. The latter file types store single data points and are useful to analyze the waveforms with another software.
Saving a waveform can be accessed via *File* → *Save* or *Save As*. The appearing window allows to select a file location and filename for the file. Different file formats such as files readable by the PicoScope software (e.g. pssettings and psdata), text files (e.g. txt and csv) and images (e.g. png and jpg) can be chosen. The options in the window allow to save only the currently displayed waveform, all waveforms in the buffer or a subset of the buffered waveforms. If not using a PicoScope file type, a separate folder will be created if multiple waveforms are saved.

The PicoScope also allows to save the waveform automatically every time the trigger fires. For saving waveforms when the trigger fires, an alarm has to be set up in the menu *Tools* → *Alarms*. In the *Alarms* dialog window, the event has to be set to *Capture* and the first item (usually it has the name *Beep*) of the list has to be selected and edited. The action is changed to *Save Current Buffer* and a directory in which the files are saved has to be chosen. It is important to set the file type explicit to a csv-file if one wants access the data points and not only obtain an image of the waveform. The stated filename will be used for all files and numbered serially. E.g. the filename is set to be *waveform*. Then the first file is *waveform.csv*, the second is *waveform (2).csv*, the third is *waveform (3).csv* etc. The set up of the alarm is finalized by closing all dialogs with

the *Save* (German: *Speichern*) or *OK* button. When starting the capturing of signals in the PicoScope software (green triangle in lower left corner), every time the trigger fires, the currently displayed waveform is stored as csv-file. To turn off the saving of pulses, it is easiest to stop the signal capture (red square in the lower left corner) and turn of the alarm in the alarm dialog window. The whole process is described in Figure C.5.

Measurements

The PicoScope allows to infer several values of the captured signals. These measurements can be used to count falling or rising edges which is useful in many experiments of the lab course whenever peaks are counted. Therefore, this introduction focuses on this measurement but counting peaks is not the only measurement featured by the PicoScope software.
A measurement is set up (c.f. Fig. C.6) via *Measurements* → *Add Measurement* (1a) or by clicking on the + on the lower menu bar (1b). In the appearing context window, multiple settings have to be set. The input channel is assigned (2). Multiple measurements of different quantities for different channels are possible. The type of measurements is defined (3) which is *Falling Edge Count* or *Rising Edge Count* if the number of peaks is supposed to be measured. It is possible to use the whole trace for a measurement or only a latter defined interval Δt (4). The measurement options allow either a threshold to be defined or an automatic threshold to be used (5). The hysteresis can be leaved unchanged. This parameter is linked to a mechanism that prevents wrongly counts due to fluctuations of the signal near the threshold. More information on that are provided in the PicoScope user's manual. If the options to use the whole trace and an automatic threshold, the measurement is ready to start. Otherwise, the rulers on the horizontal and vertical axis have to be adjusted to determine the measurement range and the threshold, respectively (c.f. Fig. C.7). The values can either by typed in the ruler legend or defined by dragging the rulers to the desired position. The measurement is found at the bottom with multiple values shown.

- The used *Channel* and *Measurement mode* are shown.
- The *Value* refers to the counted edges in the currently displayed waveform.
- The values *Min* and *Max* show the minimum and maximum counted edges, respectively, in a waveform.
- The *Average* is defined by the arithmetic average of the counts in the waveforms.
- The standard deviation σ is defined by $\sigma^2 = \frac{1}{N-1}\sum_{i=1}^{N}(y_i - \bar{y})^2$ where N is the number of captured samples, y_i the number of edges in the i-th sample and $\bar{y}$ the mean of counted edges over all samples.
- The *Capture Count* determines how many captured samples are considered. More samples result in better statistics but need more time to be collected. In case the number of captured samples exceeds the *Capture Count*, every new samples replaces the oldest considered sample. Consequently, the other values such as *Min* and *Max* only refer to the currently considered samples and not to all samples ever

captured. The *Capture Count* can be changed at *Tools* → *Preferences* → *General* → *Measurement Statistics*.
- The *Span* shows if a ruler-defined Δt is used or the whole trace.

In Section **??** a description is provided on how to access the measured values automatically.
Note that a measurement can fail which is displayed by - - in the overview of the measurement results. This problem can usually be solved by either decreasing the *Collection Time* or by reducing the *Number of Samples*. Which solution is better depends on the context of the measurement but if using the latter solution one should check that the sampling interval is still large enough to capture the signals.
Note: When using large *Collection Times* ($\geq$ 100 ms/div), the PicoScope has to be hindered to go into the *Slow Sampling Mode* otherwise wrong measurement results are obtained. This is achieved at *Tools* → *Preferences* → *Sampling* → *Slow Sampling Transition*. Here, a *Collection Time* larger than the one used in the measurement has to be chosen.

Math Channel

The PicoScope software features *Math Channels* which allow to manipulate one or multiple inputs with mathematical expressions. The output is displayed as an additional waveform in the scope and can also be used as an input channel for measurements.
Math Channels are accessed via *Tools* → *Math Channels*. The featured built-in operations are inverting the signal, adding, subtracting, multiplying and dividing two signals. It is also possible to define functions by clicking on *Create* in the *Math Channel* menu and entering the desired expression.
An application of *Math Channels* is the implementation of a coincidence counter. Two input channels which are assumed to be 0 V by default, i.e. in the digital LOW state, and have a non-zero voltage if they are in the digital HIGH state are multiplied. Only if both channel are in the digital HIGH state, the function has a non-zero output which is an implemented logical OR gate. In order to count the number of coinciding events, a measurement counting the rising or falling edges of the function can be used.

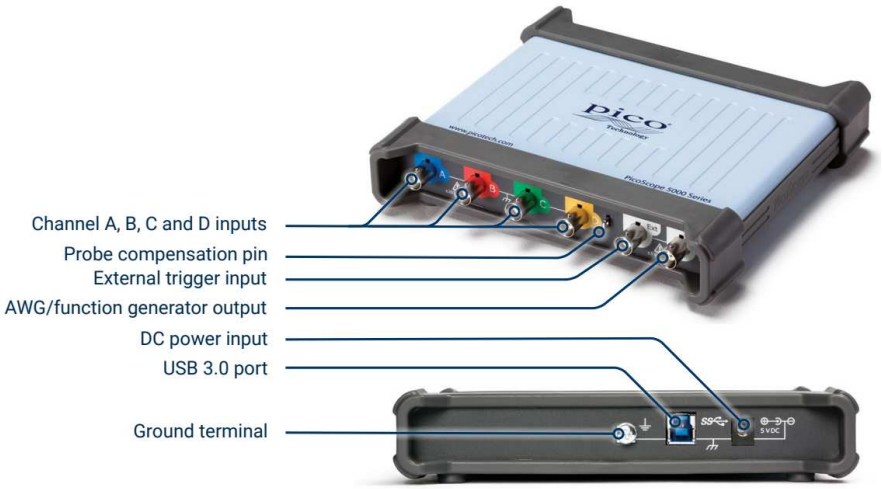

Figure C.1.: An overview over the inputs and outputs of a four channel PicoScope. Source.

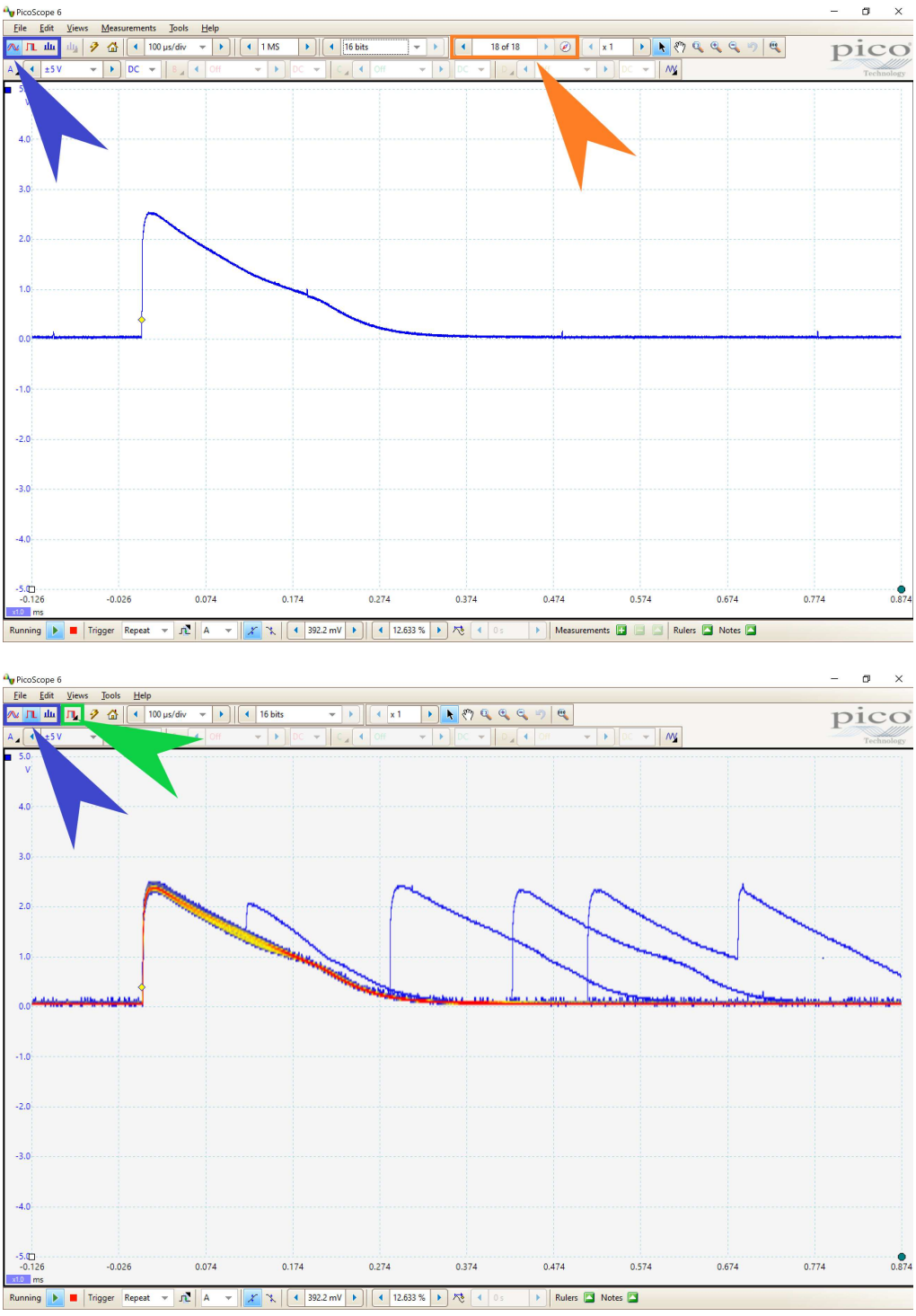

Figure C.2.: Displaying the signal in the *Scope Mode* (top) and *Persistence Mode* (bottom). The blue arrows indicate where the view modes can be accessed. The orange arrow shows the menu for the buffered waveforms and the green arrow marks the options for the *Persistence Mode*. A trigger has been in both view modes.

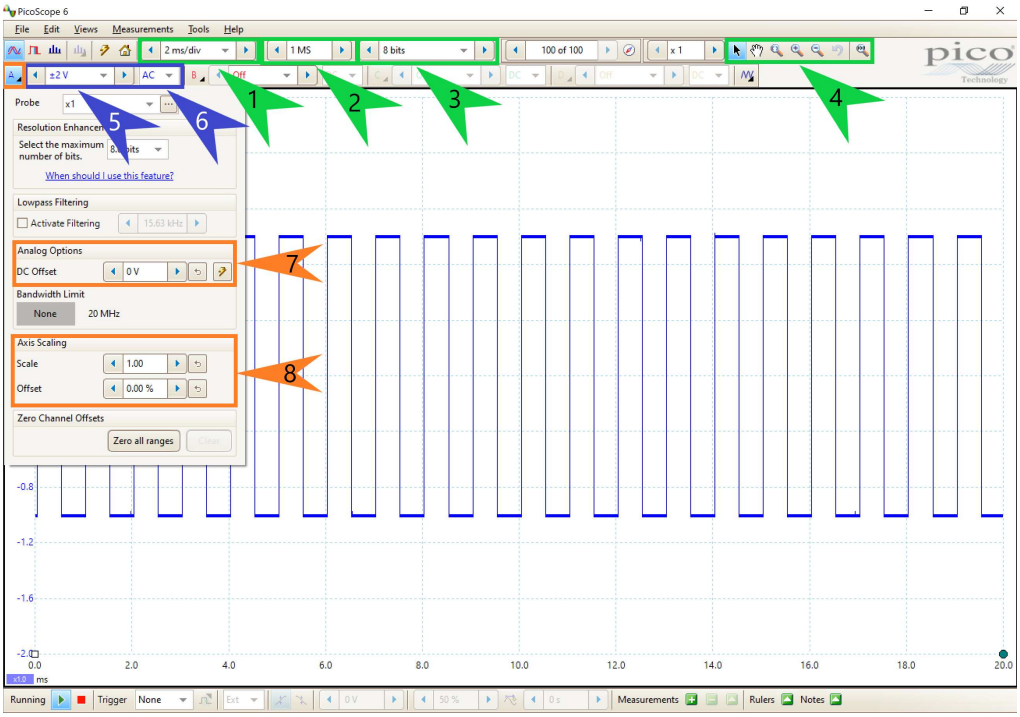

Figure C.3.: Options to modify the display of signals. THe *Scope Mode* is used. Further information can be found in the text.

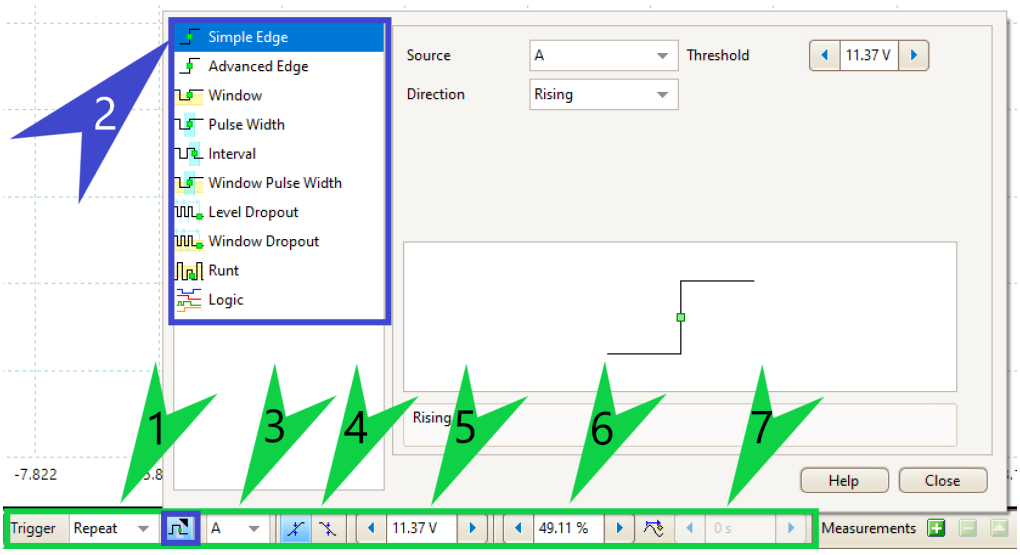

Figure C.4.: Trigger menu (green) at the bottom of the PicoScope menu. The context menu of the *Advanced Triggers* (blue) is shown. Further information can be found in the text.

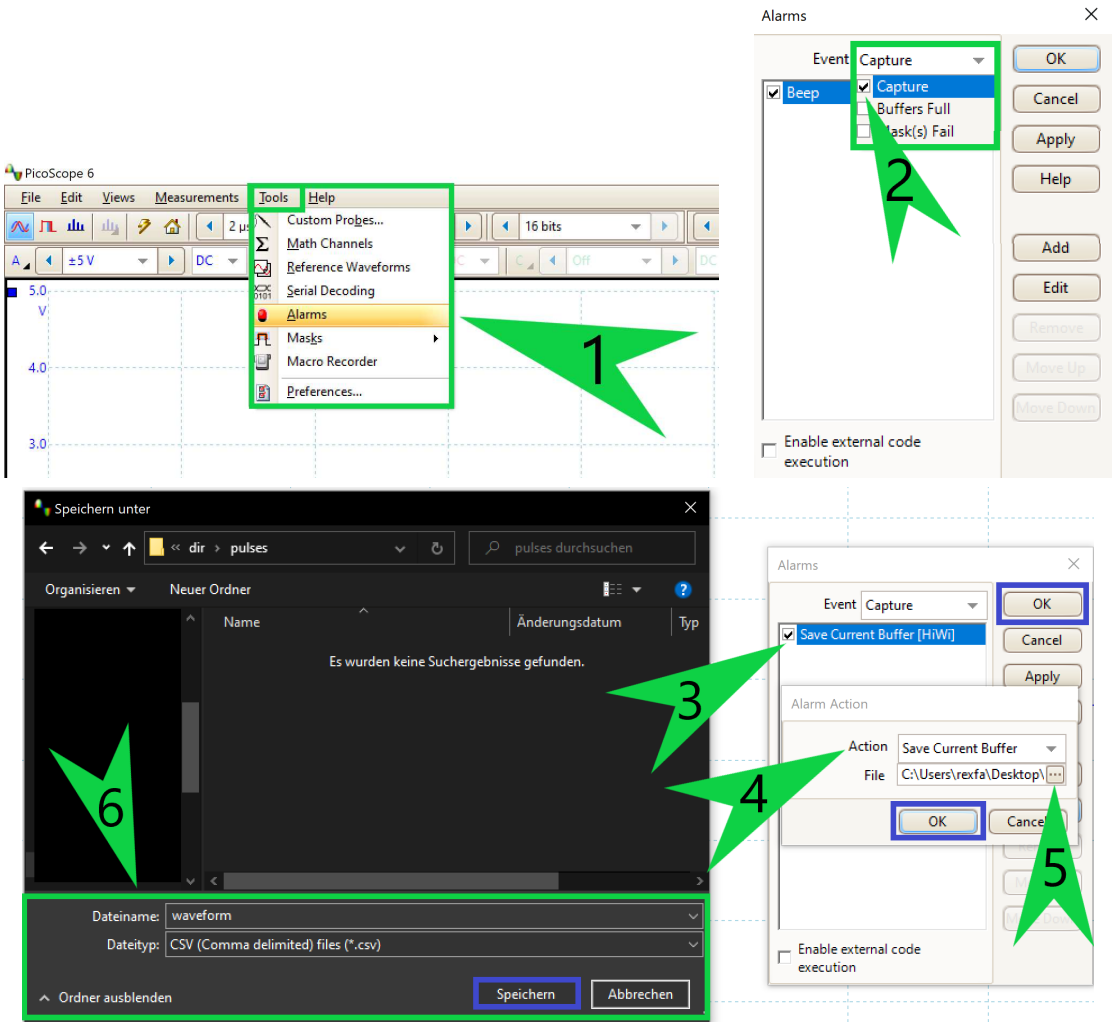

Figure C.5.: Saving pulses on trigger. In the *Alarm* dialog window (1), *Capture* has to selected as event by checking the tick box (2). A new dialog window is opened (lower image) by editing the item in the list (3). The action is set to *Save Current Buffer* (4) and the directory, filename and file type are specified (5, 6) in the next dialog window. The file type should be set to csv if the data is analysed with another software afterwards. At last, all windows are closed (blue boxes).

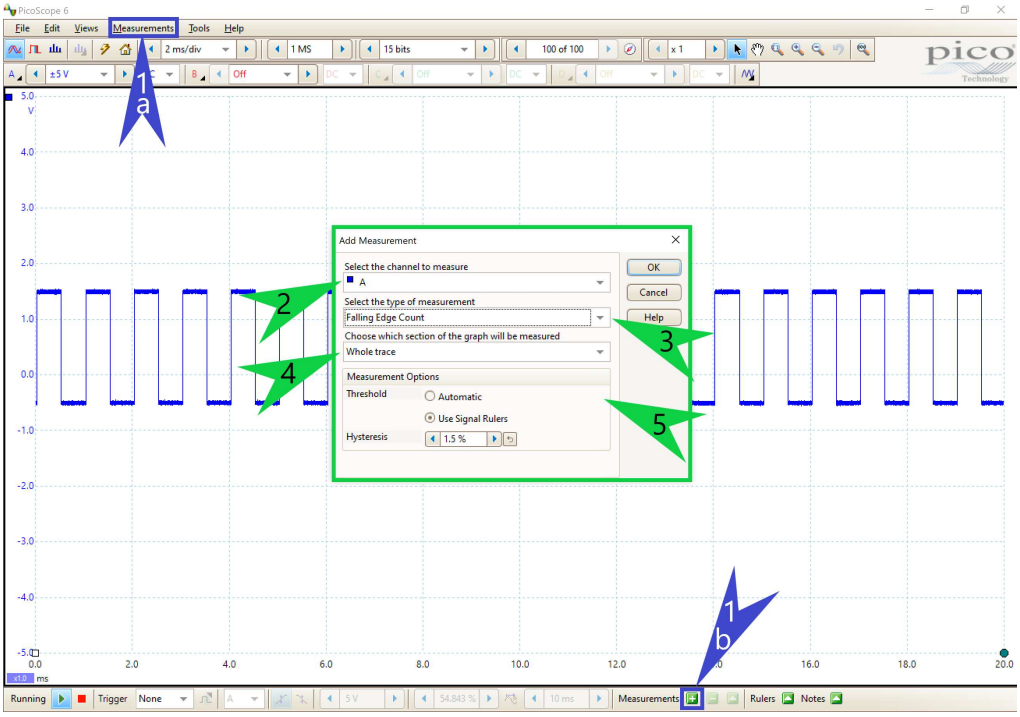

Figure C.6.: The measurement window (green frame) is opened via the menus indicated by the blue arrows. Further information can be found in the text.

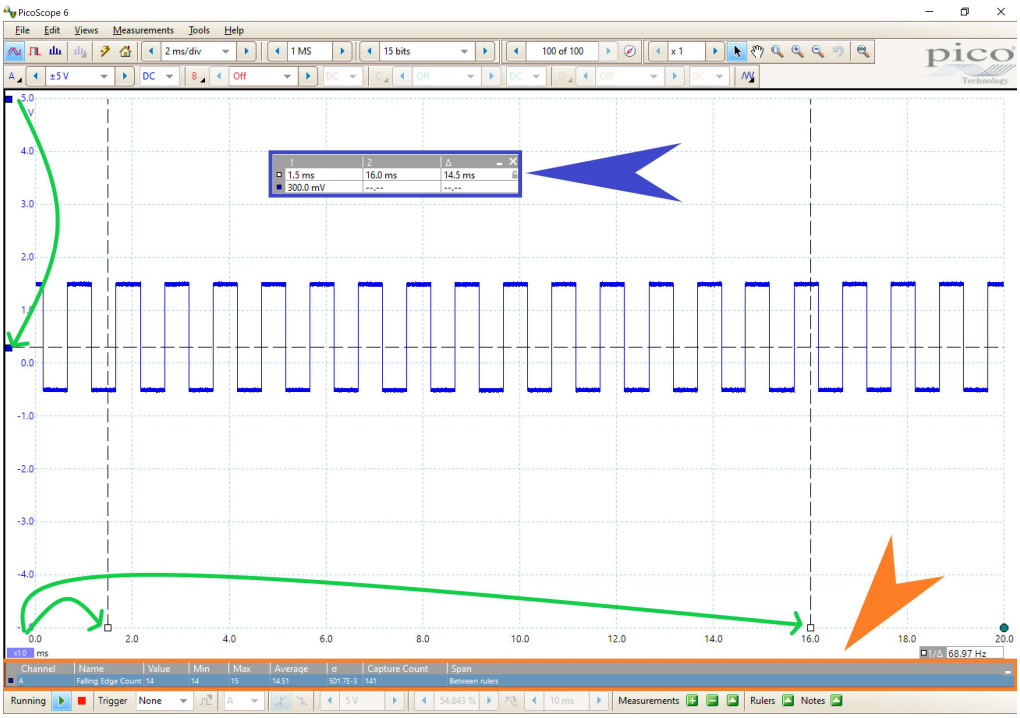

Figure C.7.: Finalizing the measurement by adjusting the ruler (green arrows) or using the ruler legend (blue arrow). The measurement results are displayed at the bottom (orange arrow). Further information can be found in the text.